

Coherence properties of high-gain twin beams generated in pump-depletion regime

A. Allevi,^{1,*} O. Jedrkiewicz,² E. Brambilla,¹ A. Gatti,² J. Peřina, Jr.,³ O. Haderka,³ and M. Bondani²

¹*Dipartimento di Scienza e Alta Tecnologia, Università degli Studi dell'Insubria and CNISM UdR Como, Via Valleggio 11, I-22100 Como, Italy,*

²*Istituto di Fotonica e Nanotecnologie, Consiglio Nazionale delle Ricerche and CNISM UdR Como, Via Valleggio 11, I-22100 Como, Italy,*

³*RCPTM, Joint Laboratory of Optics of Palacký University and Institute of Physics of Academy of Sciences of the Czech Republic, Faculty of Science, Palacký University, 17.listopadu 12, 77146 Olomouc, Czech Republic*

Twin-beam coherence properties are analyzed both in the spatial and spectral domains at high-gain regime including pump depletion. The increase of the size of intensity auto- and cross-correlation areas at increasing pump power is replaced by a decrease in the pump depletion regime. This effect is interpreted as a progressive loss in the mode selection occurring at high-gain amplification. The experimental determination of the number of spatio-spectral modes from $g^{(2)}$ -function measurements confirms this explanation.

PACS numbers: 42.65.Lm Parametric down conversion and production of entangled photons, 42.65.-k Nonlinear optics, 42.50.Ar Photon statistics and coherence theory, 85.60.Gz Photodetectors

The process of parametric down-conversion (PDC) in bulk nonlinear crystals generates twin-beam states of light that are naturally multi-mode both in spectrum and space [1]. Many works, performed in the single-photon regime, have highlighted the correlations and coherence properties of photon pairs either in spectrum or space [2–9]. In the past ten years, also high-gain PDC, leading to a large number of photons per mode, has been the object of several studies for its interesting properties of sub-shot-noise spatial intensity correlations [10–13] and macroscopic entanglement [14–19]. More recently, the spectral features of macroscopic twin-beam states have been investigated in the collinear interaction geometry close to frequency degeneracy [20]. Moreover, in the high-gain regime, the X-shaped coherence of the PDC output field [21] and the X-shaped spatio-temporal twin beam near-field correlations [22–24], originating from the space-time coupling in the phase-matching, have been demonstrated. The high-gain PDC process is also in the focus of attention for its potential applications. For instance, high-gain PDC has been used for quantum imaging [25], ghost imaging [26], and absolute calibration of photo-detectors [27, 28]. The possibility to involve such bright states in interactions with material quantum objects (atoms, molecules, quantum dots) has been also addressed. Also the application of twin beams to quantum memories has been recently suggested [29].

In this paper, we present a joint investigation of spatial and spectral features of twin-beam states produced in the high-gain regime with non-negligible pump depletion. The coherence properties at different values of pump mean power are inferred by evaluating the intensity auto- and cross-correlation functions on single-shot images of the far-field (θ, λ) speckle-like pattern of the PDC radiation. The initial increase with PDC gain of the size of coherence areas, both in spectrum and space, gradually stops and, at a certain pump power, is replaced by a decrease. This behavior is due to the occurrence of a progressive pump depletion, which is testified by the evolution of the spatial and spectral pump beam profiles. A possible explanation can be given in terms of the varying population of Schmidt paired modes [30] that ‘diagonalize’ the nonlinear interaction. The number of effectively populated modes is experimentally accessed by the measurement of spatio-spectral intensity $g^{(2)}$ -correlation function.

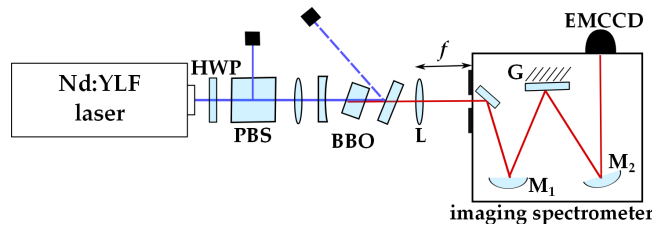


Figure 1: (Color online) Experimental setup used for the spatio-spectral measurements of the twin beam. HWP: half-wave plate; PBS: polarizing cube beam splitter; BBO: nonlinear crystal; L: lens, with 60-mm focal length; M_j : spherical mirrors; G: grating; EMCCD: electron-multiplying camera.

The experimental setup used for the measurement of the PDC light structure in the angular and spectral (θ, λ) domain is shown in Fig. 1. A type-I 8 mm-long β -Barium-Borate (BBO) crystal (cut angle = 37 deg) was pumped by the third-harmonic pulses (349 nm, 4.5-ps pulse duration) of a mode-locked Nd:YLF laser (High-Q-Laser), regeneratively amplified at 500 Hz. The crystal was tuned to have phase-matching at frequency degeneracy in quasi-collinear configuration. The pump mean power was changed by means of a half-wave plate followed by a polarizing cube beam splitter. The broadband PDC light was collected by a 60-mm focal length lens and focused on the plane of the vertical slit of an imaging spectrometer (Lot Oriel) having a 600 lines/mm

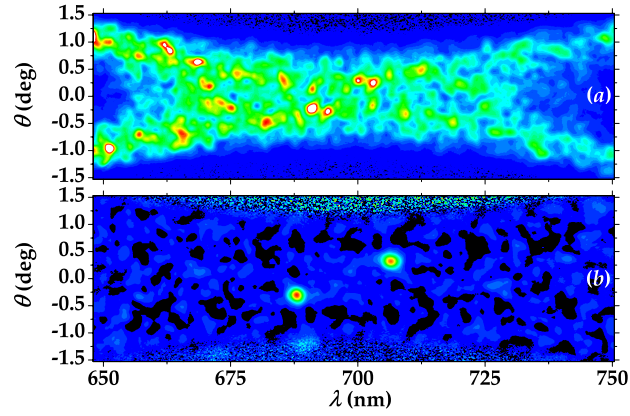


Figure 2: (Color online) (a) Single-shot image recorded by the EMCCD camera, in which the typical speckle-like pattern of PDC in the spatio-spectral domain is clearly evident. (b) Typical example of the correlation matrix $\Gamma_{k,l}^{(i,j)}$, in which the auto- and cross-correlation areas are clearly evident on the left and on the right side, respectively.

grating. The angularly dispersed far-field radiation was then recorded in single shot by a synchronized EMCCD camera (iXon Ultra 897, Andor), operated at full frame resolution (512x512 pixels, 16- μm pixel size). A typical speckle-like pattern recorded in the quasi-collinear phase-matching configuration is shown in Fig. 2(a). The existence of intensity correlations between the signal and idler portions of the twin beam is well-supported by the presence of symmetrical speckles around the degenerate wavelength and the collinear direction.

The evolution of the patterns at different pump mean powers, and hence at different PDC gains, was investigated by calculating

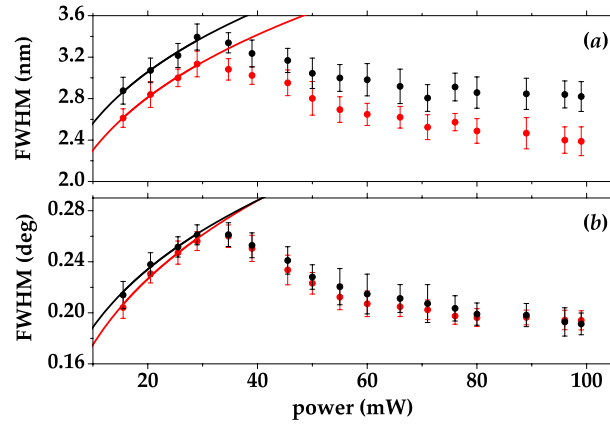


Figure 3: (Color online) Evolutions of the spectral (a) and spatial (b) FWHM size of the second-order auto-correlation (red circles) and cross-correlation (black circles) functions measured from the (θ, λ) spectra of the twin beam as functions of the pump mean power. A fourth-square root function, as expected from the theory of PDC structure under the assumption of un-depleted pump beam, is used to fit the first part of each data set.

the spatio-spectral intensity correlation function between a single pixel at coordinates (i, j) and all the pixels (k, l) contained in a single image

$$\Gamma_{k,l}^{(i,j)} = \frac{\langle I_{i,j} I_{k,l} \rangle}{\langle I_{i,j} \rangle \langle I_{k,l} \rangle}, \quad (1)$$

where I is the intensity value of each pixel expressed in digital numbers and upon subtraction of the mean value of the noise measured with the camera in perfect dark, whereas $\langle \dots \rangle$ indicates the averaging over a sequence of 1000 subsequent images. The procedure was applied to a set of pixels having the abscissa i close to frequency degeneracy and the ordinate j in the quasi-collinear direction. The function $\Gamma_{k,l}^{(i,j)}$ defined in Eq. (1) is a matrix having the same size as the original images and containing

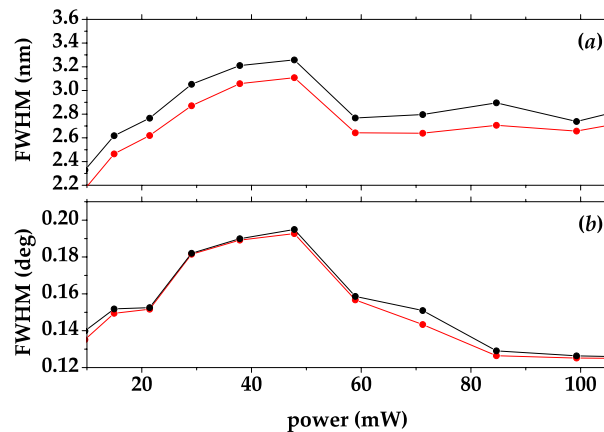


Figure 4: (Color online) Simulations of the evolution of the spectral (a) and spatial (b) FWHM size of the second-order auto-correlation (red circles+line) and cross-correlation (black circles+line) functions of the twin beam as functions of the pump mean power. See the text for details.

both the auto- and the cross-correlation areas (see Fig. 2(b)). The horizontal section of these correlation areas is related to spectrum, whereas the vertical section gives information about the angular dispersion. In Fig. 3 we show the behaviors of the spatial, *i.e.* in angular domain, (a) and spectral (b) widths, full width at half maximum (FWHM), of the intensity auto-correlation and cross-correlation profiles, as functions of the input pump mean power. In both panels, we can observe an initial growth that reaches the maximum at a pump power of about 30 mW and then decreases. As shown in the figure, only the first part of the data is well described by a fourth-root square function of pump power, as predicted by the theory of coherence areas under the assumption of un-depleted pump beam [12, 17, 26]. The second part of our experimental results (including the peak and the decrease in the FWHM) clearly indicates that the assumption of un-depleted pump beam does not hold anymore. In such a situation, also the pump beam evolves nontrivially and the corresponding equations of motion for three-mode interaction can be solved only numerically. In fact, the behavior shown in Fig. 3 is qualitatively reproduced by the numerical simulations presented in Fig. 4. These results have been obtained by means of a full 3D+1 (three spatial dimensions + time) numerical modelling of the optical system based on a pseudospectral (split-step) integration method of the nonlinear propagation equations [17]. We notice that the slight discrepancy between the absolute values of the experimental FWHMs and those obtained from simulations is mainly due to the uncertainty in the correct positioning of the EMCCD camera in the imaging exit plane of the spectrometer.

The experimental confirmation of the occurrence of pump depletion is given by the evolution of the spectral and spatial pump-beam profiles shown in the panels of Fig. 5. We obtained a spectral profile of the pump by producing a magnified image of the near field of the pump on the slit of the spectrometer and using a CCD camera (DCU223M, Thorlabs, 1024x768 pixels, 4.65- μ m pixel size) to collect the light at the output. Figure 5(a) displays different sections, normalized at their peaks, corresponding to different pump mean power values. First of all, we observe that the spectrum of the pump turns out to be ~ 1 nm wide, despite the longer pulse duration of the non-transform-limited pump beam. Secondly, we note that both the dips in the sections of panel (a) and the progressive appearance of a central hole in the contour plots shown in panels (b)-(d) are a clear signature of pump depletion. The sections of the spatial profiles presented in Fig. 5(e) and normalized at their area were obtained by taking 1:1 images of the pump beam at the output of the crystal with the same DCU223M camera at different values of the power. Also in this case a clear dip occurs. It becomes broader and deeper as the pump mean power increases. Its generation is initially slightly lateral with respect to the center because of the pump beam walk-off inside the crystal [see panels (f)-(h)].

The depletion of the pump is also responsible for the evolution of the total number of photons generated in each realization of the PDC process. In Fig. 6 we plot the mean number of photons detected in an area close to frequency degeneracy and in the quasi-collinear interaction geometry as a function of the square root of the pump peak power per pulse. To obtain this result, we have taken into account the calibration of the camera sensitivity (5.4 electrons per digital number), its detection efficiency ($\sim 90\%$ at 698 nm) and all the optical losses. The mean number of photons shown in Fig. 6 starts increasing exponentially, as expected for high-gain PDC under the hypothesis of un-depleted pump beam. This initial behavior is emphasized in the inset of the same picture, where the experimental data corresponding to the lowest pump power values are presented together with the fitting curve function, $y = A \sinh^2(Bx)$. The fitted values of A and B have been used to calculate the red curve shown in the main figure, which represents the expected gain behavior in the absence of pump depletion. In this condition, the gain of the process would vary from 5.3 up to 13.4, but the occurrence of a progressive depletion process prevents the exponential growth.

The qualitative change in the evolution of the mean number of photons, as well as of the size of coherence areas, due to pump

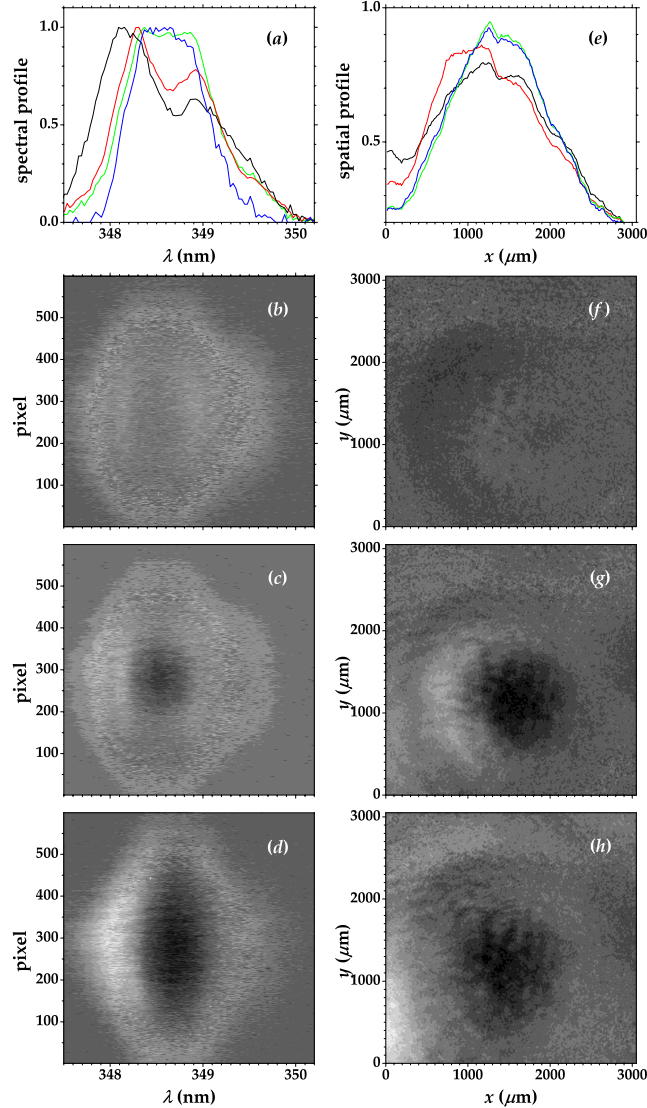


Figure 5: (Color online) Spectral and spatial pump beam profiles for different values of the pump mean power. (a): sections of the spectral profile at different pump powers (blue: 15 mW, green: 35 mW, red 55 mW and black 99 mW), (b)-(d): maps of the spectral distributions upon subtraction of the distribution of the least intense measurement ((b) 35 mW, (c) 55 mW and (d) 99 mW), (e): sections of the spatial profile at different pump powers (blue: 15 mW, green: 35 mW, red 55 mW and black 99 mW), (f)-(h): maps of the spatial distributions upon subtraction of the distribution of the least intense measurement.

depletion can be described in terms of the modes of radiation field. When the PDC process occurs at gain values leading to depletion, also the pump beam evolves in the nonlinear interaction and the dynamics of the system becomes more complex. In particular, there is a dependence of the number of effectively populated signal and idler radiation modes on the pump power. As the pump power increases, the PDC gain profile becomes narrower and narrower, and thus signal and idler fields are dominantly emitted into a smaller and smaller number of modes that gain energy to the detriment of the others [31, 32]. For sufficiently high values of the pump power, the process of mode selection reverts as the pump profile undergoes depletion. For this reason, the gain of the high-populated low-order modes is on the one side reduced, whereas the gain of low-populated higher-order modes is on the other side supported. Such a behavior explains the narrowing of the spatio-spectral correlation areas shown in Fig. 3. The description in terms of populated radiation modes also explains the slight discrepancy between auto- and cross-correlation intensity functions plotted in Fig. 3. In fact, cross-correlation function reflects the mutual coherence between signal and idler and originates in the pairwise PDC emission, whereas auto-correlation function expresses the internal coherence due to the presence of three evolving fields. As such, it is more sensitive to losses in the modes selection [33].

To give a quantitative evaluation of such modes, we consider the well-established theory of PDC at single-photon level,

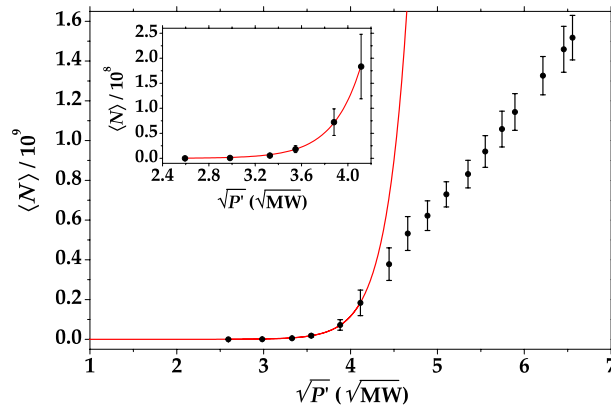


Figure 6: (Color online) Evolution of the number of photons generated by PDC as a function of the square root of the pump peak power P' per pulse. The theoretical curve (red line) holding under the assumption of an un-depleted pump beam is also shown. Inset: First part of the data shown in the main figure (black circles) together with the fitting curve predicted by the theory (red line).

according to which a bipartite state of biphotons can be written as a sum of factorized terms [30, 34] $|\Psi_{12}\rangle = \sum_k \sqrt{\lambda_k} |u_k\rangle |v_k\rangle$. Here, $|u_k\rangle$ and $|v_k\rangle$ represent the eigenvectors of a complete and orthonormal dual basis (the so-called Schmidt modes), and λ_k are the corresponding eigenvalues. We note that the number of significant eigenvalues, defined as the Schmidt number or cooperativity parameter, $K = 1/\sum_k \lambda_k^2$, quantifies the entanglement of the system. For more intense fields, the definition of cooperativity parameter K is still valid provided that we replace parameters λ_k by actual occupation probabilities of photons in mode k [35, 36]. Using this definition, the parameter K can easily be determined from the normally-ordered second-order intensity auto-correlation function $g^{(2)}$ [37], along the formula

$$g^{(2)} = 1 + 1/K. \quad (2)$$

We remark that in the macroscopic regime $g^{(2)}$ has the same expression for detected photons, thus allowing the experimental access to the correlation function [1]. In Fig. 7(a) we present the dependence of the maximum values of spatio-spectral auto- and cross-correlation functions on increasing values of the pump mean power. We note that the functions are evaluated both in the signal (colored full circles) and idler arms (colored empty circles). As already observed in Fig. 3 for the size of the auto- and cross-correlation areas, the plots exhibit a peak for the pump power of 30 mW, that lies at the beginning of the pump depletion regime. Using Eq. (2) for auto-correlation function $g^{(2)}$, we estimate the number K of modes, as shown in Fig. 7(b). The comparison of Figs. 3 and 7(b) confirms the complementary behavior of sizes of spatio-spectral areas and numbers of modes. Also a close similarity between the number K of modes assigned to the signal and to the idler arms is noticeable. At low pump powers, where no filters were used to attenuate the light of twin beams, the numbers K are nearly identical. We note that the dual basis revealed in the Schmidt decomposition [38, 39] can successfully be replaced for more intense fields by the input-output eigenmodes of the Bloch-Messiah reduction of the signal-idler unitary evolution operators [36].

In conclusion, we have presented an experimental investigation of the spatio-spectral properties of PDC in the high-gain regime including pump depletion. The evolution of the pump is responsible for the qualitative change in the size of auto- and cross-correlation areas for increasing pump power. While the correlation areas gradually broaden for lower pump power values, they undergo narrowing at increasing high pump powers. We explain this behavior by the change in the number of effectively-populated paired modes, whose complementary behavior compared to the sizes of correlation areas has been experimentally confirmed. These results provide a clear evidence that the properties of nonlinear processes at high intensities reflect a complex internal mode structure, which is on the contrary well-known for fields with intensities at the single-photon level. Work is in progress to develop a suitable detailed theoretical model that will be very useful to reach a deeper insight into the nonlinear process.

This work was supported by MIUR under the grant agreement FIRB LiCHIS - RBFR10YQ3H. JP and OH acknowledge projects P205/12/0382 of GA ĀR and projects CZ.1.05/2.1.00/03.0058 and CZ.1.07/2.3.00/20.0058 of MŠMT ĀR. OJ thanks Paolo Di Trapani for fruitful discussions.

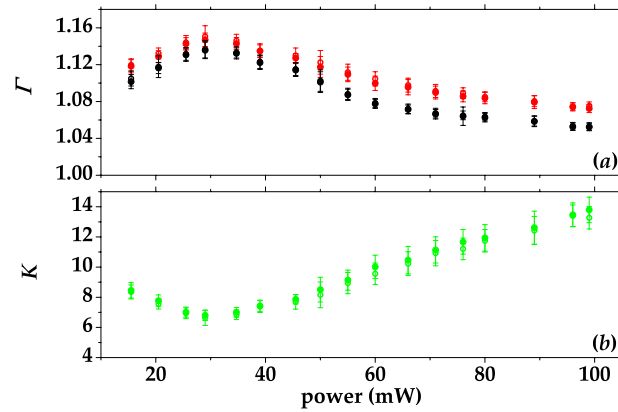


Figure 7: (Color online) (a): peak intensity of the spatio-spectral auto-correlation (red circles) and cross-correlation (black circles) functions as a function of the pump power. (b): number K of spatio-spectral modes determined from $g^{(2)}$ -intensity correlation function. In both panels the data shown as full (empty) circles characterize the signal (idler) arm.

* Electronic address: alessia.allevi@uninsubria.it

- [1] A. Allevi, S. Olivares, and M. Bondani, Phys. Rev. A **85**, 063835 (2012).
- [2] M. Hamar, J. Peřina Jr., O. Haderka, and V. Michálek, Phys. Rev. A **81**, 043827 (2010).
- [3] J.-L. Blanchet, F. Devaux, L. Furfaro, and E. Lantz, Phys. Rev. Lett. **101**, 233604 (2008).
- [4] P. A. Moreau, J. Margin-Sisini, F. Devaux, and E. Lantz, Phys. Rev. A **86**, 010101 (2012).
- [5] B. Dayan, A. Peer, A. A. Friesem, and Y. Silberberg, Phys. Rev. Lett. **94**, 043602 (2005); A. Peer, B. Dayan, A. A. Friesem, and Y. Silberberg, Phys. Rev. Lett. **94**, 073601 (2005).
- [6] K. A. O'Donnell and A. B. U'Ren, Phys. Rev. Lett. **103**, 123602 (2009).
- [7] S. Sensarn, G. Y. Yin, and S. E. Harris, Phys. Rev. Lett. **104**, 253602 (2010).
- [8] O. Haderka, J. Peřina Jr., M. Hamar, and J. Peřina, Phys. Rev. A **71**, 033815 (2005).
- [9] J. Peřina Jr., M. Hamar, V. Michálek, and O. Haderka, Phys. Rev. A **85**, 023816 (2012).
- [10] O. Jedrkiewicz, Y.-K. Yang, E. Brambilla, A. Gatti, M. Bache, L. Lugiato and P. Di Trapani, Phys. Rev. Lett. **93**, 243601 (2004).
- [11] M. Bondani, A. Allevi, G. Zambra, M. G. A. Paris, and A. Andreoni, Phys. Rev. A **76**, 013833 (2007).
- [12] G. Brida, L. Caspani, A. Gatti, M. Genovese, A. Meda, I. Ruo-Berchera, Phys. Rev. Lett. **102**, 213602 (2009).
- [13] I. N. Agafonov, M. V. Chekhova, and G. Leuchs, Phys. Rev. A **82**, 011801(R) (2010).
- [14] W. J. Munro and M. D. Reid, Phys. Rev. A **47**, 4412 (1993).
- [15] C. Simon and D. Bouwmeester, Phys. Rev. Lett. **91**, 053601 (2003).
- [16] A. Gatti, R. Zambrini, M. San Miguel and L. A. Lugiato, Phys. Rev. A **68**, 053807 (2003).
- [17] E. Brambilla, A. Gatti, M. Bache, and L. A. Lugiato, Phys. Rev. A **69**, 023802 (2004).
- [18] T. Iskhakov, M. V. Chekhova, and G. Leuchs, Phys. Rev. Lett. **102**, 183602 (2009).
- [19] C. Vitelli, N. Spagnolo, L. Toffoli, F. Sciarrino, and F. De Martini, Phys. Rev. A **81**, 032123 (2010).
- [20] K. Yu. Spasibko, T. Sh. Iskhakov, and M. V. Chekhova, Opt. Express **20**, 7507 (2012).
- [21] O. Jedrkiewicz, A. Picozzi, M. Clerici, D. Faccio, and P. Di Trapani, Phys. Rev. Lett. **97**, 243903 (2006)
- [22] A. Gatti, E. Brambilla, L. Caspani, O. Jedrkiewicz, and L. A. Lugiato, Phys. Rev. Lett. **102**, 223601 (2009).
- [23] O. Jedrkiewicz, J.-L. Blanchet, E. Brambilla, P. Di Trapani, and A. Gatti, Phys. Rev. Lett. **108**, 253904 (2012).
- [24] O. Jedrkiewicz, A. Gatti, E. Brambilla, and P. di Trapani, Phys. Rev. Lett. **109**, 243901 (2012).
- [25] G. Brida, M. Genovese, and I. Ruo Berchera, Nat. Photonics **4**, 227 (2010).
- [26] M. Bondani, A. Allevi, and A. Andreoni, Eur. Phys. J. Special Topics **203**, 151 (2012).
- [27] G. Brida, I. P. Degiovanni, M. Genovese, M. L. Rastello, and I. Ruo-Berchera, Opt. Express **18**, 20572 (2010).
- [28] I. N. Agafonov et al., Opt. Lett. **36**, 1329 (2011).
- [29] L. V. Gerasimov, I. M. Sokolov, D. V. Kupriyanov, and M. D. Havey, J. Phys. B: At. Mol. Opt. Phys. **45**, 124012 (2012).
- [30] C. K. Law and J. H. Eberly, Phys. Rev. Lett. **92**, 127903 (2004).
- [31] W. Wasilewski, A. I. Lvovsky, K. Banaszek, and C. Radzewicz, Phys. Rev. A **73**, 063819 (2006).
- [32] A. M. Perez, T. Sh. Iskhakov, P. Sharapova, S. Lemieux, O. V. Tikhonova, M. V. Chekhova, and G. Leuchs, arXiv:1402.2771 (2014).
- [33] R. Machulka, O. Haderka, J. Peřina Jr., M. Lamperti, A. Allevi, and M. Bondani, submitted.
- [34] A. Christ, K. Laiho, A. Eckstein, K. N. Cassemiro and C. Silberhorn, New J. of Phys. **13**, 033027 (2011).
- [35] A. Gatti, T. Corti, E. Brambilla, and D. B. Horoshko, Phys. Rev. A **86**, 053803 (2012).
- [36] J. Peřina Jr., Phys. Rev. A **87**, 013833 (2013).

- [37] J. Peřina, *Quantum Statistics of Linear and Nonlinear Optical Phenomena* (Kluwer, Dordrecht, 1991).
- [38] S. S. Straupe, D. P. Ivanov, A. A. Kalinkin, I. B. Bobrov, and S. P. Kulik, Phys. Rev. A **83**, 060302(R) (2011).
- [39] A. Avella, M. Gramegna, A. Shurupov, G. Brida, M. Chekhova, and M. Genovese, Phys. Rev. A **89**, 023808 (2014).